Progress in NUCLEAR SCIENCE and TECHNOLOGY, Vol. 2, pp.247-252 (2011)

ARTICLE

Efficient Calculation of *in vivo* Efficiency Curves Using Variance Reduction Techniques

Jad FARAH, David BROGGIO* and Didier FRANCK

Institut de Radioprotection et de Sureté Nucléaire, IRSN/DRPH/SDI/LEDI, BP-17 92260 Fontenay-aux-Roses Cedex, France

To optimize the *in vivo* lung monitoring of nuclear workers, realistic calibration coefficients are assessed using 3D anthropomorphic models and Monte Carlo simulations. In this study, a Livermore voxel phantom and the torso of the ICRP adult female reference voxel phantom were used. Monte Carlo MCNPX simulations were achieved to compute the calibration curve for a typical germanium counting system with a photon source of energy ranging from 15 keV to 1.4 MeV. However, photons of low energy are highly attenuated by body compounds while high energy photons are too penetrative to interact in the detectors. Hence, statistically insufficient counting efficiency values are obtained for both energy ranges. Thus, MCNPX variance reduction techniques were considered here to accelerate the simulations. The variance reduction techniques used were: the source biasing to favor low energy emissions; the emission direction biasing to select emission towards detectors; the forced collision to improve high energy photons interaction in germanium active cells. These techniques reduced the computing time by a factor of 20 and improved the associated statistical error with no significant variation in counting efficiency. Cell importance, mesh tally, weight windows and exponential transform variance reduction techniques were also tested to further accelerate computation.

KEYWORDS: in vivo monitoring, counting efficiency, voxelized phantoms, Monte Carlo, variance reduction, computation time

I. Introduction

In case of internal contamination risks, *in vivo* counting is a very useful method for the monitoring of workers and for estimating the incorporated activity for X and Gamma emitters. For routine measurements, calibration coefficients are generally assessed using physical models, like the Livermore phantom,[1-2] of known source activity and distribution. To go towards a more realistic calibration, voxelized phantoms associated to Monte Carlo (MC) calculations have proven to be the most promising solution.[3-4] However, MC simulations are time consuming depending on the complexity of the input file, particularly the way the phantom, the source and the detectors are coded with voxel grids. To define realistic models of the human body, millions of voxels are required. For example, the ICRP adult female reference voxelized model consists of 3.9 million voxels.[5] Simulations also depend on the nature of the requested output data, namely the number and nature of the tallies (MC results), and the cells in which the score is recorded. Thus, calculations of several hours or even days can sometimes be required to obtain a statistically acceptable MC result. The aim of this work was to reduce the duration of the simulations and to improve the statistics using MC Variance Reduction (VR) techniques.[6]

This paper is divided in two sections. The first section introduces the *in vivo* monitoring problematic and MC simulations. The definition, assessment, uncertainties and dependency of counting efficiency are first presented. Then, MCNPX simulation entries and results are given and discussed for two voxelized phantoms.[7] The second section deals with improving counting efficiency simulations by the use of VR. First, several VR techniques are listed with indications on their aim, input parameters and functioning. Then, the results of using such VR are given and discussed particularly in terms of the simulation time reduction, the counting efficiency values and the associated statistical relative error.

*Corresponding author, E-mail: david.broggio@irsn.fr

II. Counting Efficiency and MC Simulations

In vivo monitoring is based on spectrometry measurements to estimate the incorporated activity. This requires the use of dedicated counting systems. Typical calibration coefficients are assessed using physical phantoms and real measurements or via Monte Carlo simulations associated to realistic voxelized phantoms.[3,4] Using these calibration coefficients, i.e. counting efficiency, the retained activity can be deduced from the measured counting rate.

1. Counting Efficiency

(1) Definition

Counting efficiency (ε) is the fundamental quantity characterizing an *in vivo* counting system and is defined, for a given measurement, as follows:

$$\tau_{\exp} = \varepsilon . y_i A \quad (1)$$

where τ_{exp} is the experimental counting rate [counts/s], y_i the emission yield of the studied gamma radiation [photon/nuclear disintegration] and A the activity [Bq]. Here, and

according to definition, counting efficiency is given in counts/gamma. It is the ratio of the number of detected particles to the total number of starting particles for a given photoelectric peak and a precise energy.

(2) Assessment

To assess in vivo counting efficiency, the energy spectrum measured by the detectors needs to be processed. Counting efficiency is obtained from the counting rate by analyzing the full energy peak. However, the latter often grows on the Compton continuum which needs to be subtracted from the final value of the peak (cf. **Fig. 1**). For the conducted simulations, no Gaussian Energy Broadening (GEB) factor was used. Therefore, the counting efficiency is directly deduced from the height of the photoelectric peak from which the Compton socket, estimated through the mean value of the two channels to the left and to the right of the peak, is subtracted.

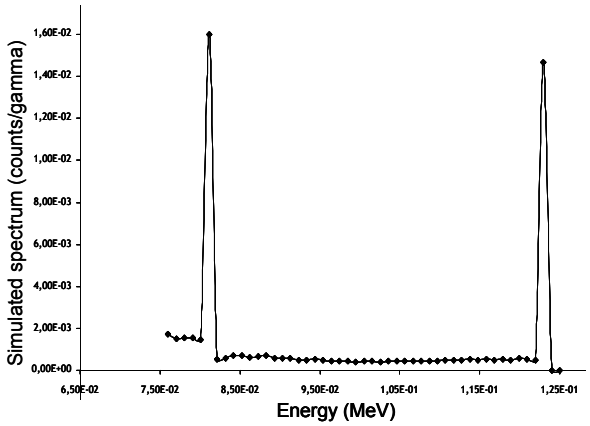

Fig. 1. Simulated spectrum (counts/gamma) reported for two photons of 81 and 122 keV. Left photoelectric peak growing on its own Compton spectrum and on that of the right photoelectric peak.

(3) Uncertainties

When calibrating a counting system, the uncertainty on counting efficiency can be as low as 5%.[8)] However, when applying these calibration coefficients to a routine measurement, the uncertainty on the assessed activity can be up to 50%.[8-10)] Type B errors, on the distribution of activity within the body for example or on the subject positioning during *in vivo* measurement, are predominant in uncertainty calculation. This uncertainty is assessed from the scattering factor.[8)] Nevertheless, voxel phantoms are more realistic when representing the human body. Simulations aim to reduce uncertainties, and particularly the Type B uncertainties on the phantom, and values of 5 to 10% are considered satisfactory, particularly for low energy photons, when compared to the 50% measurement error.

For MCNPX simulations, counting efficiency is assessed using an f8 type tally that represents the pulse height tally for the active cells of the detectors. For such a tally, results are acceptable only if the associated statistical relative error is less than 5%. However, the simulated counting efficiency value is calculated by considering the Compton bins surrounding the photoelectric peak (cf. Section I. 1. (2)). For these bins, the 5% simulation statistical relative error is not guaranteed. Thus, the error on the final counting efficiency can be assessed on the large side by using the following equation:

$$\sigma_{\varepsilon_{ff}} = \sqrt{(\sigma_{peak})^2 + (\sigma_{peak-1})^2 + (\sigma_{peak+1})^2} \qquad (2)$$

where σ_{peak} is the uncertainty of the bin reproducing the photoelectric peak while σ_{peak-1} and σ_{peak+1} represent such an uncertainty for the bins surrounding the peak and corresponding to Compton contribution. Each σ weights the MC statistical relative error with the number of counts (spectrum height) for each bin. For high energy photons (> 100 keV), the Compton counts are negligible when compared to the photoelectric peak and thus the overall uncertainty is roughly equivalent to that of the photoelectric peak (no more than 5%). For low energy photons, however, similar counts are observed for both the Compton and the photoelectric bins and thus uncertainty is assessed using Eq. (2) with a maximum acceptable value of 9%.

(4) Dependency

Counting efficiency is directly affected by the:

- Phantom (or patient) and particularly the morphology, size, tissue composition and density.
- Source nature (photons, electron, neutrons etc.), the emission energy and distribution.
- Detectors positioning, number of channels, sensibility of the detection crystals and the GEB parameters.

Simulations take into account these parameters to reproduce realistic measurements.

2. MCNPX Simulations

The MCNPX input file was generated using the OEDIPE software and by specifying the detectors, the phantoms and the source to reproduce a typical *in vivo* pulmonary measurement.[11)]

In this study, the counting system used for the simulations was that of the AREVA La Hague medical analysis department. This system consists of 4 germanium detectors that were modeled and validated in a previous study.[12)] The detectors were positioned as close as possible to the body to cover at best the lungs, with a tilt of 35° along the head-to-foot axis for the female phantom to prevent any collision between detectors and breasts. The considered number of channels for these detectors was 16,384 and no GEB card was used.

Moreover, the phantoms used were two voxelized models, created from CT scan images, representing the Livermore physical phantom and the torso of the ICRP Adult Female Reference Computational Phantom (ICRP AF-RCP).[5)] The two models have totally different number of segmented organs (5 for the Livermore and 67 for the female phantom), different tissue composition and density (tissue equivalent plastic for the Livermore) and different voxels both in number (7.7 *vs.* 2.2 million voxels for the Livermore and the female phantoms respectively) and in dimensions (8E-03 *vs.* 15E-03 cm^3 for the Livermore and the female phantoms re-

spectively). These phantoms were included in the MC input file section using the repeated structures format that had been proven to be more efficient to accelerate the simulations.[13)]

Finally, the source used in this work was an artificial gamma source emitting 17 different emissions of energies ranging from 15 keV (for ^{238}U) to 1.4 MeV (for ^{152}Eu). This source simulated the radionuclides most commonly used for calibrating detectors dedicated for *in vivo* monitoring. A uniform distribution of 1 Bq of this source was operated in the lung volume.

All simulations were conducted using MCNPX 2.6c.[6)] The total number of simulated particles (NPS) was the same for the Livermore and the female simulations. NPS was set to 1E09 particles that were equally divided into the 17 different gamma emissions. Such a high number of simulated particles was taken to ensure an acceptable statistical relative error (< 5%) for all the simulated photons particularly those of 15 keV. The output includes the requested tally values, the simulation time and complementary values like the figure of merit, the interaction tables (collisions, absorption, fluorescence etc.), the statistical analyses results etc.

3. MCNPX Simulation Results

Table 1 summarizes the results obtained for the Livermore phantom and the ICRP female model for six energies. The simulation time was roughly equal to 7 days for the Livermore voxelized phantom while it was around 6 days for the female model. These are the reference results obtained for simulations with no applied VR.

Figure 2 represents the variation of the simulated counting efficiency with energy for the female phantom and the germanium detectors presented above. Similar variation was found for the Livermore phantom.

The uncertainty values of Table 1 were calculated following Eq. (2). For the 15 keV photons and the female phantom for example, the uncertainty was obtained as follows. The photoelectric peak height was around 1.2E-04 counts/gamma while its MC statistical relative error was about 1.2%. However, the surrounding Compton bins were about 7.2E-05 and 6.8E-05 counts/gamma with statistical relative error values of 1.5% and 1.6% respectively. These were deduced from the final counting efficiency that was evaluated at 4.52E-05 counts/gamma and gave an uncertainty value of 4.61%.

Table 1 Simulated counting efficiency and associated uncertainty for the Livermore and the female phantoms

Phantom	Livermore		ICRP female	
Radionuclide	Count Eff. (counts/γ)	Unc. (%)	Count Eff. (counts/γ)	Unc. (%)
^{238}U (15 keV)	6.03E-05	3.37	4.52E-05	4.61
^{241}Am (59 keV)	1.15E-02	0.12	1.29E-02	0.12
^{57}Co (122 keV)	1.31E-02	0.11	1.47E-02	0.11
^{152}Eu (244 keV)	8.76E-03	0.14	1.01E-02	0.13
^{137}Cs (661 keV)	3.62E-03	0.22	4.33E-03	0.20
^{60}Co (1.17 MeV)	2.40E-03	0.27	2.91E-03	0.24

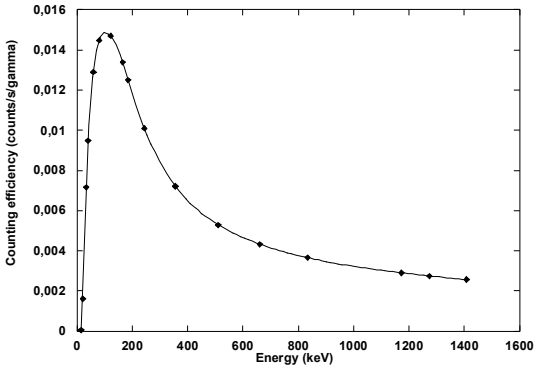

Fig. 2 Variation of simulated counting efficiency (counts/gamma) with energy (keV) for the female phantom.

4. MCNPX Simulation Discussion

The variation of MC simulated counting efficiency with energy, given in Fig. 2, represents a typical counting efficiency curve for the used detectors. The MCNPX model of the detectors and the simulation method were validated when compared to experimental measurements as similar counting efficiency values were obtained.[14)] Moreover, as it is shown in this plot, counting efficiency is highly dependent on the photon energy. Indeed, poor efficiency values were obtained for low energy photons that are highly attenuated by body tissue. The efficiency values were also low for high energy photons that are too penetrative to interact with the detectors. Meanwhile, for photons of medium energy, the particles were sufficiently energetic to go throughout the body, get to the detectors and interact. The efficiency distribution with photon energy can thus be divided into 3 regions:

- Region #1: less than 33 keV (^{139}Ce)
- Region #2: 33 keV to 350 keV (^{133}Ba)
- Region #3: more than 350 keV

Monte Carlo variance reduction techniques were thus implemented to improve the results in each region and accelerate the simulations.

III. Improving Counting Efficiency Simulation

To improve the counting, it was necessary to increase the number of low energy particles of region #1 in order to increase the probability of collecting such photons. Moreover, high energy photons of region #3 were requested to interact with the detectors. Finally, for the intermediate energy photons of region #2, the number of particles could be reduced to gain time without affecting the simulation results. These improvements were rendered possible by using VR techniques that were implemented to reduce the simulation time while preserving a correct counting efficiency value within the initial error range of 9%.

1. Variance Reduction Techniques

Variance Reduction aims to attribute more time for the particles that will most probably contribute to the final result while ignoring those of minor probability and thus reduce the total simulation time. In this paper, two categories of VR techniques were introduced: the Population Control Methods

(PCM) that controls the sampling and the Modified Sampling Methods (MSM) that bias and modify the distributions and sampling.[6-7] VR modifies the particles propagation probability and adjusts the associated weights to maintain physically coherent results.

(1) SB Card: Biasing the Distribution of Particles

The first MCNPX VR technique used was the Source Biasing card (SB), which is considered to be a MSM. This card enables the control of photon emissions and their energy distribution. The artificial source that was first used emitted an equal number of photons for all the 17 different gamma emissions. The number of photons per energy ray was equal to the total NPS (1E09) divided by the number of photons (17) that is about 5.9E07. This card was used for two applications. In the first application, the goal was to reduce the number of photons of medium and high energy, of Regions #2 and #3, and conserve the number of photons of very low energies in Region #1 particularly those of 15 keV. Using SB, 29% (15/51) of the total NPS was associated for this energy and the rest equally divided between the 16 other photons of greater energy. The second application, however, aimed to double the number of photons of 15 keV at the expense of those of Regions #2 and #3. In this case, more than 40% of the total NPS was associated with the 15 keV photons.

(2) FCL Card: Forcing the Photon Collisions

The FCL card was the second VR technique used to force the collision of photons in the active cells of the detector. This is of particular interest for the high energy emissions as previously discussed. The use of such a card required the determination of the total number of cells in the problem and the ones in which to force the collision (those of the detectors). These cells are also the ones for which the f8 tally was requested i.e. detectors active cells. For these cells, the FCL parameter was set to one, which is equivalent to a 100% collision probability, while default collision probabilities were maintained in all the other cells.

(3) VEC Card: Biasing the Emission Direction

The VEC card was introduced in this work to control the direction of the source emission (VEC for vector). All the particles going towards the back of the phantom and away from the detector have a very low, and even insignificant, probability to contribute to the count. To improve the count, an emission direction towards the detectors was applied. The probability of the photons to go in that direction or in another one was defined by the user. For this work, particles going in the negative x plan direction were severely reduced to a probability of only 1E-06 while for those going the other direction, the probability was set to 1. This type of VR should be used with caution since it significantly alters the weight of the particles if a strong biasing is applied. In fact, if a particle with low contribution probability comes to count for the requested result, its weight would be huge (1/probability=1E06) which will dramatically bias the result leading to a false convergence.

(4) EXT Card: Increasing the Mean Free Path

The EXT card was used to help the photons pass through the body tissue by increasing their mean free path. This card was used to improve the low energy photons contribution to the count. The use of such card required a weight window card to control the weight of the particles. The considered mean free path augmentation was equal to 0.9 for both the Livermore and the female simulations as recommended by the MCNPX manual.[7] This card was applied on the phantom organs and also for the dead layer of the detectors.

(5) Cell Importance: Particles Population Biasing

The MCNPX particles transportation code propagates the photons starting from the source cell and all over the working universe. A given importance is associated to each cell and is used to propagate the particles. For example, a zero importance cell would mean that all particles entering this cell are killed. The fate of a particle depends on the importance ratio between the entered and the exited cells. If this ratio is higher than one, the primary particle is divided, using the "Splitting" function,[6] into as many daughter particles as the value of the ratio. The weight of the daughter particles is set to be equal to the primal weight divided by the number of daughter particles. In the case where the ratio is less than 1, "Russian roulette" is played to fuse particles of identical energy and their weight is added.[6]

For these simulations, the importance associated to the different cells was tripled when moving from one organ (one cell number) to another and doubled when getting to the detectors. Namely, and for the Livermore simulations, the lung (source organ) importance was set to 1, the importance of residual tissue and bones was set to 3. Finally, the importance of chest wall plate was set to 9 while it was set to 18 for detectors.

2. Variance Reduction Results

Table 2 shows the number of simulated particles required to guarantee statistically reliable MC values (error < 5%).

Table 3 gives the simulation time reduction obtained with different applied variance reduction techniques for both the Livermore and the ICRP female phantoms. Moreover, **Table 4** gives the simulated efficiency values in counts/gamma and the associated differences (in %), obtained for the 15 keV ^{238}U photons, when compared to the reference values (without VR). The VR cards were implemented by combining progressively each card with another. For example in the

Table 2 Number of simulated particles for the applied VR techniques to save time and guarantee reliable MC values

Simulation	REF	SB	FCL*	VEC*	EXT*	IMP*
NPS	1E09	1.5E08	1.5E08	7E07	7E07	2E07

Table 3 Gain of simulation time for the applied VR simulations with the voxelized Livermore phantom compared with the reference simulations without VR

Time reduction	SB	FCL	VEC	EXT	IMP
Livermore	10.7	10.4	20.6	19.5	22.5
ICRP female	10.6	10.6	19.8	18.2	21.2

Table 4 Simulated counting efficiency (counts/γ) for the applied VR methods and the associated difference (%) compared with the reference values obtained for 238U and both phantoms (Livermore and the ICRP female)

Phantom	Livermore		ICRP female	
VR method	Count Eff. (counts/γ)	Diff. (%)	Count Eff. (counts/γ)	Diff. (%)
SB	5.92E-05	1.9	4.68E-05	-3.5
FCL	6.25E-05	-3.6	4.63E-05	-2.5
VEC	6.34E-05	-5.2	4.35E-05	3.8
EXT	6.26E-05	-3.9	4.53E-05	-0.2
IMP	6.07E-05	-0.6	3.60E-05	20.0

tables below, FCL* refers to the association of SB and FCL, VEC* is the combination of SB, FCL and VEC, EXT* is the sum of the three previous cards and EXT and finally IMP* is the combination of SB, FCL, VEC and the Cell Importance card.

3. Variance Reduction Discussion

It is clear from Table 3 that similar time gain was obtained for both the Livermore and the ICRP female phantoms regardless of the multiple differences existing between the models (cf. Section II. 2. (1)). Moreover, Table 4 shows that the difference between counting efficiency values and the reference ones (without VR) remained acceptable when considering the rough 9% uncertainty which was mainly due to the Compton deduction (cf. Section II. 1. (3)). However, for higher energy photons, the maximum relative error between the VR efficiencies and the reference ones was less than 3%. Below is a detailed discussion of the effect of each VR card.

(1) SB Card Effect

The SB card was first used to increase the number of photons of Region #1 to the detriment of those of Regions #2 and #3. When compared to the reference efficiency values, obtained without any VR, the Livermore voxelized phantom simulations showed an agreement within 1.9% when the same number of particles was simulated for the ^{238}U photons of 15 keV (cf. Table 4). For the female phantom, the maximum observed difference was about -3.5% for the same energy (cf. Table 4). Moreover, when the number of particles of such an energy was doubled, the difference to the reference value was quite the same. However, the associated statistical relative error was reduced from 3% to 2% at 15 keV for the Livermore model and from 3.3% to 2.4% for the female phantom at the same energy. These observations confirm the efficiency of increasing the number of low-energy particles in order to improve the counting efficiency in Region #1 by using the SB card. The time reduction was almost the same (10.6) regardless of the complexity of the phantom (Livermore *vs*. ICRP female phantom). This gain is mainly due to the significant reduction of the NPS in Region #2. Indeed, in this region, the number of particles was reduced from about 5.9E07 particles (1E09/17) for each photon of a given energy to only about 3.9E06 particles maintaining, however, a good statistical relative error of less than 0.4% for all photons of Region #2.

(2) FCL Card Effect

The FCL card decreased the statistical error of high energy photons more than it reduced the simulation time. Such a card is easy to use and implement since the only required entry is the cell number in which to force the collision. The maximum difference observed for high energy photons between the reference simulation and the new one with FCL, was reduced from -1.4% (SB card only) to -1.1% (SB and FCL cards combined) with the Livermore simulations and the ^{22}Na photon of 1.27 MeV; and from -1% (SB) to -0.05% (SB+FCL) with the female ones concerning the same gamma radiation. The relative statistical error was reduced for the high energy photons from 0.1% (SB) to 0.07% (SB+FCL) for the Livermore phantom and the ^{152}Eu photon of 1.4 MeV. For the female phantom, the relative statistical error was reduced from 0.9% (SB) to 0.6% (SB+FCL) for the same photon.

(3) VEC Card Effect

The VEC card was used to bias the direction of the source emission. This was done by using a 180° angle to favor emissions towards the detectors and a factor 2 time gain was obtained. The efficiency values remained in agreement with the primal ones since acceptable differences were observed considering the 9% uncertainty and the Compton participation. However, angular biases of smaller values were also tested to further increase the time reduction. This gave unsatisfying results since differences in efficiency values of up to 20% were obtained when compared to the reference values. This can be explained by the scattered radiations and the fact that the emission direction biasing is towards one particular point. As a matter of fact, choosing the emission direction vector does not imply the same biasing for all photons especially since the source is distributed in the lung volume and not punctual.

(4) EXT Card Effect

The application of the Exponential Transform card is much more difficult than the previous ones since it requires the use of Weight Windows to control the weight of the generated particles that can be significantly modified by this card. The use of this card was particularly interesting since it reduced the difference in counting efficiency from values greater than 5% for the Livermore simulations (VEC), and the 15 keV photon, to a lower error value of only 3.9%. When considering the simulation time reduction, this card was however of poor result since particles were propagated for longer tracks. Moreover, to use this card, multiple iterations were required to generate the optimal weight windows, which was considerably time consuming.

(5) IMP Card Effect

The manual modification of the cells importance reduced both the simulation time and the total NPS required for these simulations (cf. Tables 2 and 3). The NPS was divided by the same factor, 3, as cells importance was tripled between the phantom organs. This card saved simulation time of a factor 1.1 when compared to the VEC simulation. From Table 4, it can be deduced that using such card can be more delicate when the number of cells increases (case of the fe-

male phantom). Indeed, the relative error in counting efficiency is much higher when comparing the Livermore model (67 cells) to the female phantom (198 cells). More adequate cell importance assigning can be found but remain, however, strictly based on essay-error tests.

(6) Hardware

To further reduce the MC simulation time, a parallel version of the code was used to launch the transport of particles on 32 processors at the same time. This nearly reduced the total simulation time by a factor of 20 that adds up to the previous time gain to generate a total time reduction by a factor of 400 for the VEC simulation in the case of the Livermore phantom.

IV. Conclusion

The monitoring of workers with internal contamination risks is done by *in vivo* spectrometry measurements. Routine calibration of the counting systems is done using physical phantoms. MC simulations, however, are useful for more realistic numerical calibrations. This work highlights the use of such simulations to assess counting efficiency calibration curves and focuses on speeding up the calculations.

Accelerating the counting efficiency assessment was done by minimizing the simulation time using variance reduction techniques (VR). The applied VR techniques were the source biasing, the emission direction biasing, the forced collision, weight windows associated to exponential transform parameters and the cell importance. These enabled a final time reduction by a factor of 20 (400 when considering parallel simulations). The obtained counting efficiency values agreed within 5% for the 15 keV photons and 1% for photons of higher energy when compared to reference simulations. The VR also improved the MC statistics particularly for high energy photons with the FCL card and low energy photons with the EXT card. The obtained results confirmed that the efficiency of each VR techniques depend mainly on the energy of the simulated particles. However, when considering the differences between the used phantoms, the obtained results showed that simulation time depends on the number of voxels rather than on the material of those voxels. Indeed, with a simple phantom like the Livermore model, with only 5 different structures, the simulation time reduction, obtained by using VR, was equal to the one obtained with the female complex phantom of 67 structures.

As a future step, new VR techniques can be tested such as the DXTRAN spheres for deterministic transport of particles or the RDUM card for emission direction biasing towards a fictitious sphere covering the detectors. The work will also focus on simplifying the geometry of the phantom and on reducing the total number of voxels to study the impact on the simulation time and on counting efficiency.

Acknowledgment

This work was carried out as part of PIC DOSINTER, a collaboration project between AREVA and IRSN.

References

1) D.Newton, A. C. Wells, S. Mizushita, R. E. Toohey, J. Y. Sha, R. Jones, S. J. Jefferies, H. E. Palmer, G. A. Rieksts, A. L. Anderson, G. W. Campbell, *The Livermore Phantom as a Calibration Standard in the Assessment of Plutonium in Lungs. Assessment of Radioactive Contamination in Man*, STI/PUB/674, IAEA, Vienna (1985).
2) R. V. Griffith, P. N. Dean, A. L. Anderson, J. C. Fisher "Fabrication of a tissue-equivalent torso phantom for intercalibration of in-vivo transuranic-nuclide counting facilities," *Symp. Adv. Radiat. Prot. Monit.*, Stockholm (1978).
3) D. Franck, N. Borissov, L. de Carlan, N. Pierrat, J. L. Genicot, G. Etherington, "Application of Monte Carlo calculations to calibration of anthropomorphic phantoms used for activity assessment of actinides in lungs," *Radiat. Prot. Dosim.*, **105**, 403-408 (2003).
4) G. H. Kramer, L. C. Burns, K. S. Thind,"Monte Carlo simulations: A useful tool to extend in vivo calibrations and explore alternative approaches," *Radiat. Prot. Dosim.*, **105**[1-4], 553-556 (2003).
5) International Commission on Radiological Protection,"ICRP Publication 110: Adult Reference computational phantoms," *Ann. ICRP* **39**[2] (2009).
6) T. E. Booth, *A sample problem for Variance Reduction*, LA-10363-MS, Los Alamos National Laboratory (LANL) (1985).
7) D. B. Pelowitz (ed), *MCNPX User's manual version 2.6.0*, LA-CP-07-1473, Los Alamos National Laboratory (LANL) (2008).
8) H. Doerfel, A. Andrasi, M. Bailey, V. Berkovski, E. Blanchardon, C. M. Castellani, C. Hurtgen, B. LeGuen, I. Malatova, J. Marsh, J. Stather, *General guidelines for the estimation of Committed Effective Dose from incorporation monitoring data*, Project IDEAS-EU Contract No. FIKR-CT2001-00160 (2006).
9) M. Schlagbauer, *Calibration and uncertainty budget analyses for a whole body counter in scan geometry using physical and numerical phantoms*, Graz University of Technology (2006).
10) N. Razafindralambo, *Limite de détection de la spectrométrie X pour l'anthroporadiamétrie pulmonaire du plutonium : Analyse et perspectives de développement*. Mémoire de Thèse, Université Paul Sabatier (1995).
11) D. Franck, L. de Carlan, N. Pierrat, D. Broggio, S. Lamart "OEDIPE: a new graphical user interface for fast construction of numerical phantoms and MCNP calculations," *Radiat. Prot. Dosim.* **127**[1–4], 262–265 (2007).
12) S. Lamart, *Etude de l'influence de la biocinétique des radionucléides sur la mesure anthroporadiamétrique à l'aide de fantômes numériques voxélisés*. Mémoire de Thèse, Université Paris-Sud 11 (2008).
13) S. Chiavassa, *Développement d'un outil dosimétrique personnalisé pour la radioprotection en contamination interne et la radiothérapie vectorisée en médecine nucléaire*. Mémoire de Thèse, Université Paul Sabatier (2005).
14) J. Farah, D. Broggio, D. Franck, "Female workers and in vivo lung monitoring: a simple model for morphological dependency of counting efficiency curves," *Phys. Med. Biol.*, **55**, 7377-7395 (2010).